

Magnetic field-induced chiral soliton lattice in the bulk magnetoelectric helimagnet Cu_2OSeO_3

Cite as: J. Appl. Phys. **138**, 103905 (2025); doi: [10.1063/5.0289322](https://doi.org/10.1063/5.0289322)

Submitted: 7 July 2025 · Accepted: 25 August 2025 ·

Published Online: 9 September 2025



Victor Ukleev,^{1,2,a)}  Arnaud Magrez,³  and Jonathan S. White¹ 

AFFILIATIONS

¹Laboratory for Neutron Scattering and Imaging (LNS), PSI Center for Neutron and Muon Sciences, Villigen PSI, CH-5232 Switzerland

²Helmholtz-Zentrum Berlin für Materialien und Energie, D-14109 Berlin, Germany

³Crystal Growth Facility, Institute of Physics, École Polytechnique Fédérale de Lausanne, CH-1015 Lausanne, Switzerland

^{a)}Author to whom correspondence should be addressed: victor.ukleev@helmholtz-berlin.de

ABSTRACT

Chiral soliton lattices (CSLs) are anharmonic magnetic structures typically found in uniaxial chiral magnets. In this study, we report the observation of CSL in bulk Cu_2OSeO_3 , a chiral insulator known for its magnetoelectric properties. Using small-angle neutron scattering (SANS) experiments, we demonstrate the formation of CSLs in Cu_2OSeO_3 at low temperatures, driven by the competition between cubic anisotropy and magnetic field. Our observations of higher harmonics in the SANS signal clearly indicate the anharmonic nature of the spiral. This finding underscores the complex interplay between magnetic interactions in Cu_2OSeO_3 , offering insights for potential applications of CSLs in electric-field-controlled spintronic devices.

© 2025 Author(s). All article content, except where otherwise noted, is licensed under a Creative Commons Attribution (CC BY) license (<https://creativecommons.org/licenses/by/4.0/>). <https://doi.org/10.1063/5.0289322>

I. INTRODUCTION

The interplay of exchange and Dzyaloshinskii–Moriya interactions (DMI) and the magnetocrystalline anisotropy yields a diverse magnetic phase diagram in chiral cubic crystals, encompassing paramagnetic, helimagnetic, forced ferromagnetic, conical, and skyrmion phases.¹ Application of a magnetic field parallel to the propagation vector of a magnetic helix results in the canting of the magnetic moments toward the field direction, leading to the transformation of the helical texture into a conical state [Fig. 1(a)]. Further increments in the magnetic field result in the transition from the conical to the forced ferromagnetic state. If significant cubic anisotropy is present, a moderate magnetic field applied perpendicular to the helical propagation axis can deform the proper screw magnetic modulation into an elliptic spiral^{2,3} also known as chiral soliton lattice (CSL)⁴ [Fig. 1(a)]. However, the CSL state typically appears in uniaxial chiral magnets due to the interplay between easy-axis anisotropy and external magnetic fields,⁴ and this distorted state is often neglected for cubic systems, despite its signature has been clearly observed in the prototype *B20* compound MnSi.^{5,6} Another peculiar, multi-*k* magnetic solitonic texture that arises in chiral helimagnets under applied magnetic

fields is a skyrmion crystal, a hexagonally ordered array of topologically protected chiral magnetic vortices.^{7,8} The cubic anisotropy affects the shape of skyrmions^{9,10} and the skyrmion lattice orientation with respect to the applied field.¹¹ Furthermore, the competition between cubic and anisotropic exchange anisotropies enriches the magnetic phase diagram with tilted conical and low-temperature disordered skyrmion phases.^{12–15}

Magnetic solitons hold promise as information carriers in next-generation non-volatile memory and logic devices.¹⁶ Despite extensive theoretical investigations into the current-induced motion of CSLs in itinerant chiral magnets,^{17,18} the influence of electric (*E*–) fields has not been explored, although the formation of CSLs in insulating materials has been reported.¹⁹ The creation and manipulation of CSLs by *E*–fields offer an alternative means of controlling CSLs in insulating helimagnets.

The ground state of bulk Cu_2OSeO_3 is a proper-screw spiral with the propagation vector parallel to the $\langle 100 \rangle$ crystal axes, resulting in a multidomain zero-field state. Upon the application of a magnetic field, the system undergoes a transition from the helical to the conical or skyrmion lattice phase.²⁰ Recent experiments have demonstrated CSL stabilization in *B20*-type magnetoelectric Cu_2OSeO_3 by applying uniaxial stress or tensile strain.^{21,22}

06 October 2025 09:16:33

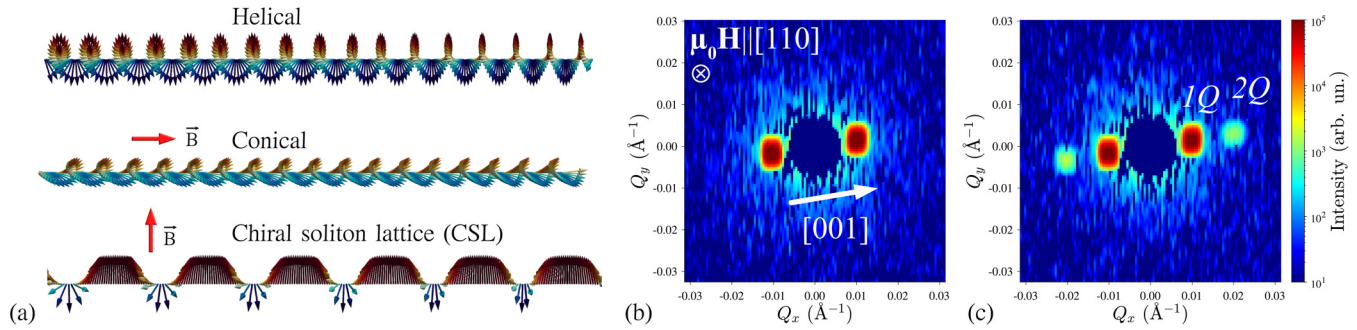


FIG. 1. (a) Schematic illustrations of spin patterns in the helical state, conical, and chiral soliton lattice (CSL) states. (b) and (c) Magnetic small-angle neutron scattering (SANS) patterns obtained at $T = 2$ K and (b) zero field and (c) $\mu_0 H = 22$ mT. First-order SANS peaks 1Q are accompanied by the higher-order satellites 2Q due to the field-induced deformation of the spiral.

Furthermore, by exploiting the magnetoelectric nature of Cu_2OSeO_3 , previous studies have demonstrated the E -field-induced phase control of chiral spin textures, such as skyrmion lattices, helical, and conical orders in bulk samples and thin plates using moderate E -fields of 5–30 kV/mm.^{23–31}

In the present paper, using small-angle neutron scattering (SANS), we demonstrate magnetic field-induced CSL formation in Cu_2OSeO_3 at low temperatures due to the cubic anisotropy and its manipulation by magnetic fields. Although most theoretical treatments of CSL formation focus on uniaxial systems, our observations show that even modest cubic anisotropy is sufficient to stabilize the CSL phase. To our knowledge, no explicit theoretical framework currently addresses this mechanism in cubic systems; however, phenomenological models such as the sine-Gordon description remain applicable. Using the observed critical field for spiral reorientation (~ 40 mT), one can estimate the anisotropy strength required to overcome the Zeeman energy, providing a rough but self-consistent validation of this mechanism in Cu_2OSeO_3 . The obtained magnetic-field dependence of the modulation vector along the [001] direction is in good agreement with the sine-Gordon theoretical model. This makes Cu_2OSeO_3 a promising material for the non-volatile manipulation of CSLs.

II. EXPERIMENTAL

For our experiments, a single crystal of Cu_2OSeO_3 was grown using a chemical vapor transport method.²⁰ We performed SANS experiments on a $3 \times 3 \times 1$ mm³ sample with the thin axis parallel to the cubic [001] direction.

The crystal was mounted onto a dedicated sample stick³² and loaded into a 7 T horizontal-field cryomagnet MA7 (Oxford Instruments, UK). We utilized a longitudinal SANS configuration with the incoming neutron's wavevector $k_i \parallel \mathbf{H} \parallel [110]$ [Fig. 1(b)].

The SANS measurements were conducted using the SANS-I setup at the Swiss Spallation Neutron Source SINQ, Paul Scherrer Institute (Villigen, Switzerland). We employed an incident neutron beam with the wavelength $\lambda = 5$ Å and the bandwidth of 10%, collimated over a distance of 18 m before the sample, and the diffracted neutrons were collected by a position-sensitive detector

(PSD) located 18 m after the sample. The SANS patterns were measured by rocking the sample and cryomagnet together through an angular range of $\pm 4^\circ$ that moved the diffraction spots through the Bragg condition at the detector with the step size of 0.5° . Background measurements were carried out in the field-polarized state at $\mu_0 H = 150$ mT and subtracted from the other datasets to emphasize the signal due to magnetic modulations. The data were analyzed using GRASP software.³³

III. RESULTS AND DISCUSSION

Figure 1(b) shows the SANS measured at $T = 2$ K and zero magnetic field after zero-field cooling (ZFC). The diffraction pattern comprises two Bragg peaks from the helical magnetic texture aligned along the [001] axis. In this geometry, diffraction arising from the other two helical domains is out of the scattering plane. Consistent with previous studies, the length of the magnetic wavevector at zero field is $Q_0 = 0.0098(1) \text{ \AA}^{-1}$, corresponding to a real-space periodicity of 64 nm. The width of the Bragg peaks is limited by the experimental resolution. The zero-field proper-screw helical state has a purely sinusoidal magnetic structure factor that results in the single Fourier harmonic seen in the SANS pattern. Upon increments of the magnetic field, the spiral acquires the net magnetization along the field direction through the elliptic deformation. Thus, the corresponding Fourier transform of the magnetization (SANS pattern) shows higher harmonics.³

Experimentally, this transformation from helical to anharmonic CSL upon the field increase is evidenced in SANS, where even a small field of 4 mT is sufficient to generate the anharmonicity and, consequently, the emergence of the second harmonic [Fig. 1(c)]. This anharmonic spiral is distinct from other modulated magnetic states in Cu_2OSeO_3 , such as the conical or skyrmion lattice phases, by the presence of higher-order harmonics in the SANS pattern and the absence of hexagonal symmetry. Observation of even higher harmonics would also be possible with a bigger sample or longer SANS acquisition times. In order to resolve fine details of the helicoidal structure in the real-space, a high-resolution coherent resonant x-ray scattering^{34,35} or Lorentz transmission electron microscopy⁴ would be required. In contrast

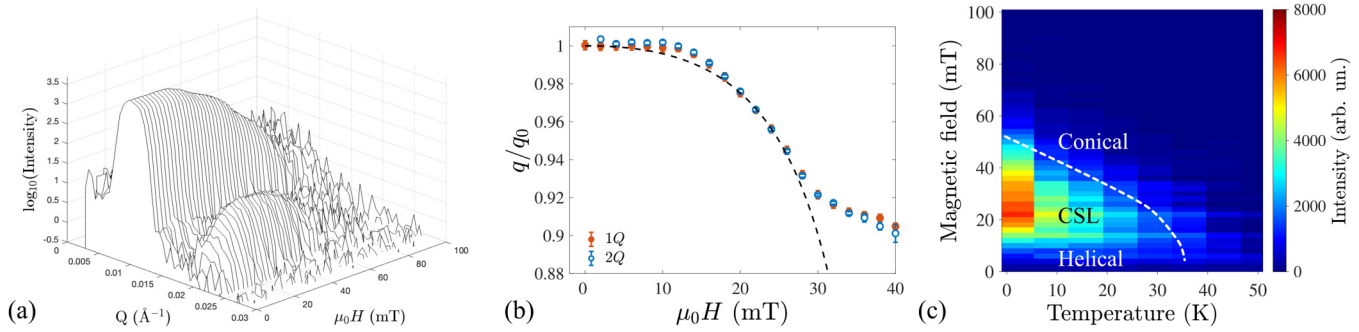


FIG. 2. (a) Waterfall plot of the integrated intensities of the SANS pattern measured at $T = 2$ K. Appearance of the second-harmonic peak at $Q \approx 0.02 \text{\AA}^{-1}$ indicates the CSL state. (b) The magnetic-field dependence of the normalized wavevector extracted from the fitted Q_1 and Q_2 peak positions. The dashed line is the fit according to the sine-Gordon model. (c) Colormap plot of the second harmonic peak intensity corresponding to the order parameter of the CSL state. Dashed line indicates the approximate boundary between the CSL and conical phases, based on the sharp drop in the 2Q harmonic intensity.

to the conical state, where a single Q -vector aligned with the magnetic field dominates, the CSL retains a nontrivial propagation vector orientation and a multi-harmonic structure, even within the coexistence range of around 30–40 mT. The transition from helical to CSL textures upon the field increase progresses up to the point when the magnitude of the field is sufficient for the re-orientation of the spiral wavevector towards the field axis (conical state). At $\mu_0 H \approx 40$ mT, the CSL almost fully transforms into the conical state with the wavevector aligned toward the magnetic field direction, which is not contributing to the SANS signal in the present geometry. The magnitude of this critical field corresponds to the energy barrier of the spiral plane flop provided by the magnetocrystalline anisotropy.

The magnetic-field dependence of the radially integrated SANS intensities at $T = 2$ K is shown in Fig. 2(a). The intensity dependence of the second harmonic at $Q \approx 0.02 \text{\AA}^{-1}$ generally follows predictions of the sine-Gordon model,³ in which the higher-harmonic intensities gradually increase with the applied magnetic field, and with the previous experimental data on the strained Cu_2OSeO_3 ²¹ and FeGe ³⁶ nanostructures, and bulk MnSi .^{5,6}

The magnetic-field dependence of the CSL normalized wavevector q/q_0 has been derived from the Gaussian fit of the integrated intensities of the SANS patterns [Fig. 2(b)]. The dependence follows the sine-Gordon law [dashed line in Fig. 2(b)] similarly to uniaxial chiral magnets if the demagnetization effect is taken into account.³⁷ However, when the field is above ~ 30 mT, and the CSL co-exists with the out-of-plane conical state, the Q -dependence clearly deviates from the theoretical trend. At this field, the anharmonic spiral with the propagation vector along [100] stabilized by the magnetocrystalline anisotropy becomes less energy favorable than the field-aligned conical state. Therefore, only metastable CSL domains survive the transition field of 30 mT, but further changes in their shapes become impossible and result in the spiral plane flop.

Finally, the intensity of the second harmonic peak 2Q is summarized in a temperature vs magnetic field map as shown in Fig. 2(c). The intensity is peaked at base temperature 2 K and the field of 22 mT and gradually vanishes at $T \sim 40$ K. Such behavior was also observed in bulk MnSi ⁵ and explained by the presence of

cubic anisotropy.³⁸ This observation also aligns well with the temperature behavior of magnetocrystalline³⁹ and exchange¹⁵ anisotropies in Cu_2OSeO_3 .

IV. CONCLUSION

In summary, our investigation delves into the stability of the chiral soliton lattice (CSL) within bulk unstrained Cu_2OSeO_3 . Utilizing small-angle neutron scattering experiments, we unveil the magnetic field-induced emergence of CSLs at low temperatures, attributed to magnetocrystalline anisotropy. The observation of higher-harmonic satellites underscores the significant anharmonicity of the helical spiral. Interestingly, Kelvin-probe force microscopy measurements²⁶ indicate the development of a finite electric polarization along the $\langle 100 \rangle$ axis at small magnetic fields applied along $\langle 110 \rangle$. This axis corresponds to the direction of the helical wavevector in the CSL state, suggesting that the observed polarization may originate from a non-collinear magnetoelectric coupling unique to the anharmonic CSL structure as it was also proposed in other magnetoelectric chiral helimagnets.^{40,41} This highlights the complexity of the interplay between electric polarization and magnetic fields and calls for further theoretical and experimental investigations to elucidate the role of anisotropic magnetoelectric coupling in shaping the CSL dynamics in Cu_2OSeO_3 .

ACKNOWLEDGMENTS

The authors thank O. I. Utesov for enlightening discussions. We thank M. Bartkowiak for experimental support. V.U., A.M., and J.S.W. acknowledge funding from the SNSF Sinergia CRSII5-171003 NanoSkyrmionics. J.S.W. also acknowledges funding from the SNSF Project No. 200021_188707. SANS measurements at the SINQ (Paul Scherrer Institut) were performed as a part of the Proposal No. 20180048.

AUTHOR DECLARATIONS

Conflict of Interest

The authors have no conflicts to disclose.

Author Contributions

Victor Ukleev: Conceptualization (lead); Data curation (lead); Formal analysis (lead); Investigation (equal); Visualization (lead); Writing – original draft (lead). **Arnaud Magrez:** Investigation (equal); Writing – review & editing (supporting). **Jonathan S. White:** Conceptualization (equal); Data curation (equal); Funding acquisition (lead); Investigation (lead); Supervision (lead); Writing – review & editing (equal).

DATA AVAILABILITY

The data that support the findings of this study are openly available in Zenodo repository (Ref. 42).

REFERENCES

- ¹Y. Tokura and N. Kanazawa, “Magnetic skyrmion materials,” *Chem. Rev.* **121**, 2857–2897 (2021).
- ²I. Dzyaloshinskii, “The theory of helicoidal structures in antiferromagnets. II. Metals,” *Sov. Phys. JETP* **20**, 223–231 (1965).
- ³Y. A. Izyumov, “Modulated, or long-periodic, magnetic structures of crystals,” *Sov. Phys. Usp.* **27**, 845–867 (1984).
- ⁴Y. Togawa, T. Koyama, K. Takayanagi, S. Mori, Y. Kousaka, J. Akimitsu, S. Nishihara, K. Inoue, A. Ovchinnikov, and J.-I. Kishine, “Chiral magnetic soliton lattice on a chiral helimagnet,” *Phys. Rev. Lett.* **108**, 107202 (2012).
- ⁵S. Grigoriev, S. Maleyev, A. Okorokov, Y. O. Chetverikov, P. Böni, R. Georgii, D. Lamago, H. Eckerlebe, and K. Pranzas, “Magnetic structure of MnSi under an applied field probed by polarized small-angle neutron scattering,” *Phys. Rev. B* **74**, 214414 (2006).
- ⁶Y. Kousaka, N. Ikeda, T. Ogura, T. Yoshii, J. Akimitsu, K. Ohishi, J.-I. Suzuki, H. Hiraka, M. Miyagawa, S. Nishihara *et al.*, “Chiral magnetic soliton lattice in MnSi,” in *Proceedings of the International Symposium on Science Explored by Ultra Slow Muon (USM2013)* (The Physical Society of Japan, 2014), p. 010205.
- ⁷S. Mühlbauer, B. Binz, F. Jonietz, C. Pfleiderer, A. Rosch, A. Neubauer, R. Georgii, and P. Böni, “Skyrmion lattice in a chiral magnet,” *Science* **323**, 915–919 (2009).
- ⁸X. Z. Yu, Y. Onose, N. Kanazawa, J. Park, J. Han, Y. Matsui, N. Nagaosa, and Y. Tokura, “Real-space observation of a two-dimensional skyrmion crystal,” *Nature* **465**, 901 (2010).
- ⁹V. Ukleev, Y. Yamasaki, D. Morikawa, K. Karube, K. Shibata, Y. Tokunaga, Y. Okamura, K. Amemiya, M. Valvidares, H. Nakao *et al.*, “Element-specific soft x-ray spectroscopy, scattering, and imaging studies of the skyrmion-hosting compound $\text{Co}_2\text{Zn}_8\text{Mn}_4$,” *Phys. Rev. B* **99**, 144408 (2019).
- ¹⁰M. Preißinger, K. Karube, D. Ehlers, B. Szigeti, H.-A. Krug von Nidda, J. White, V. Ukleev, H. Rønnow, Y. Tokunaga, A. Kikkawa *et al.*, “Vital role of magnetocrystalline anisotropy in cubic chiral skyrmion hosts,” *npj Quantum Mater.* **6**, 65 (2021).
- ¹¹T. Adams, M. Garst, A. Bauer, R. Georgii, and C. Pfleiderer, “Response of the skyrmion lattice in mnsi to cubic magnetocrystalline anisotropies,” *Phys. Rev. Lett.* **121**, 187205 (2018).
- ¹²A. Chacon, L. Heinen, M. Halder, A. Bauer, W. Simeth, S. Mühlbauer, H. Berger, M. Garst, A. Rosch, and C. Pfleiderer, “Observation of two independent skyrmion phases in a chiral magnetic material,” *Nat. Phys.* **14**, 936–941 (2018).
- ¹³F. Qian, L. J. Bannenberg, H. Wilhelm, G. Chaboussant, L. M. Debeer-Schmitt, M. P. Schmidt, A. Aqeel, T. T. Palstra, E. Brück, A. J. Lefering *et al.*, “New magnetic phase of the chiral skyrmion material Cu_2OSeO_3 ,” *Sci. Adv.* **4**, eaat7323 (2018).
- ¹⁴L. J. Bannenberg, H. Wilhelm, R. Cubitt, A. Labh, M. P. Schmidt, E. Lelièvre-Berna, C. Pappas, M. Mostovoy, and A. O. Leonov, “Multiple low-temperature skyrmionic states in a bulk chiral magnet,” *npj Quantum Mater.* **4**, 11 (2019).
- ¹⁵P. R. Baral, O. I. Utesov, C. Luo, F. Radu, A. Magrez, J. S. White, and V. Ukleev, “Direct observation of exchange anisotropy in the helimagnetic insulator Cu_2OSeO_3 ,” *Phys. Rev. Res.* **5**, L032019 (2023).
- ¹⁶T.-H. Kim, S. Cheon, and H. W. Yeom, “Switching chiral solitons for algebraic operation of topological quaternary digits,” *Nat. Phys.* **13**, 444 (2017).
- ¹⁷I. Bostrem, J.-I. Kishine, and A. Ovchinnikov, “Theory of spin current in chiral helimagnets,” *Phys. Rev. B* **78**, 064425 (2008).
- ¹⁸K. Koumpouras, A. Bergman, O. Eriksson, and D. Yudin, “A spin dynamics approach to solitons,” *Sci. Rep.* **6**, 25685 (2016).
- ¹⁹J. Schefer, M. Boehm, B. Roessli, G. Petrakovskii, B. Ouladdiaf, and U. Staub, “Soliton lattice in copper metaborate, Cu_2O_4 , in the presence of an external magnetic field,” *Appl. Phys. A* **74**, s1740–s1742 (2002).
- ²⁰S. Seki, X. Yu, S. Ishiwata, and Y. Tokura, “Observation of skyrmions in a multiferroic material,” *Science* **336**, 198–201 (2012).
- ²¹Y. Okamura, Y. Yamasaki, D. Morikawa, T. Honda, V. Ukleev, H. Nakao, Y. Murakami, K. Shibata, F. Kagawa, S. Seki *et al.*, “Emergence and magnetic-field variation of chiral-soliton lattice and skyrmion lattice in the strained helimagnet Cu_2OSeO_3 ,” *Phys. Rev. B* **96**, 174417 (2017).
- ²²T. Nakajima, V. Ukleev, K. Ohishi, H. Oike, F. Kagawa, S.-I. Seki, K. Kakurai, Y. Tokura, and T.-H. Arima, “Uniaxial-stress effects on helimagnetic orders and skyrmion lattice in Cu_2OSeO_3 ,” *J. Phys. Soc. Jpn.* **87**, 094709 (2018).
- ²³J. S. White, I. Levatić, A. Omrani, N. Egetenmeyer, K. Prša, I. Živković, J. L. Gavilano, J. Kohlbrecher, M. Bartkowiak, H. Berger *et al.*, “Electric field control of the skyrmion lattice in Cu_2OSeO_3 ,” *J. Phys.: Condens. Matter* **24**, 432201 (2012).
- ²⁴J. White, K. Prša, P. Huang, A. Omrani, I. Živković, M. Bartkowiak, H. Berger, A. Magrez, J. Gavilano, G. Nagy *et al.*, “Electric-field-induced skyrmion distortion and giant lattice rotation in the magnetoelectric insulator Cu_2OSeO_3 ,” *Phys. Rev. Lett.* **113**, 107203 (2014).
- ²⁵E. Ruff, P. Lunkenheimer, A. Loidl, H. Berger, and S. Krohns, “Magnetoelectric effects in the skyrmion host material Cu_2OSeO_3 ,” *Sci. Rep.* **5**, 15025 (2015).
- ²⁶P. Milde, E. Neuber, A. Bauer, C. Pfleiderer, H. Berger, and L. M. Eng, “Heuristic description of magnetoelectricity of Cu_2OSeO_3 ,” *Nano Lett.* **16**, 5612–5618 (2016).
- ²⁷Y. Okamura, Y. Yamasaki, D. Morikawa, T. Honda, V. Ukleev, H. Nakao, Y. Murakami, K. Shibata, F. Kagawa, S. Seki *et al.*, “Directional electric-field induced transformation from skyrmion lattice to distinct helices in multiferroic Cu_2OSeO_3 ,” *Phys. Rev. B* **95**, 184411 (2017).
- ²⁸J. White, I. Živković, A. Kruchkov, M. Bartkowiak, A. Magrez, and H. Rønnow, “Electric-field-driven topological phase switching and skyrmion-lattice metastability in magnetoelectric Cu_2OSeO_3 ,” *Phys. Rev. Appl.* **10**, 014021 (2018).
- ²⁹P. Huang, M. Cantoni, A. Kruchkov, J. Rajeswari, A. Magrez, F. Carbone, and H. M. Rønnow, “In situ electric field skyrmion creation in magnetoelectric Cu_2OSeO_3 ,” *Nano Lett.* **18**, 5167–5171 (2018).
- ³⁰P. Huang, M. Cantoni, A. Magrez, F. Carbone, and H. M. Rønnow, “Electric field writing and erasing of skyrmions in magnetoelectric Cu_2OSeO_3 with an ultralow energy barrier,” *Nanoscale* **14**, 16655–16660 (2022).
- ³¹M.-G. Han, F. Camino, P. A. Vorobyev, J. Garlow, R. Rov, T. Söhnel, J. Seidel, M. Mostovoy, O. A. Tretiakov, and Y. Zhu, “Hysteretic responses of skyrmion lattices to electric fields in magnetoelectric Cu_2OSeO_3 ,” *Nano Lett.* **23**, 7143–7149 (2023).
- ³²M. Bartkowiak, J. White, H. M. Rønnow, and K. Prša, “Note: Versatile sample stick for neutron scattering experiments in high electric fields,” *Rev. Sci. Instrum.* **85**, 026112 (2014).
- ³³C. Dewhurst, “Graphical reduction and analysis small-angle neutron scattering program: GRASP,” *J. Appl. Crystallogr.* **56**, 1595–1609 (2023).
- ³⁴V. Ukleev, Y. Yamasaki, D. Morikawa, N. Kanazawa, Y. Okamura, H. Nakao, Y. Tokura, and T.-H. Arima, “Coherent resonant soft x-ray scattering study of magnetic textures in FeGe,” *Quantum Beam Sci.* **2**, 3 (2018).

- ³⁵C. Tabata, Y. Yamasaki, Y. Yokoyama, R. Takagi, T. Honda, Y. Kousaka, J. Akimitsu, and H. Nakao, "Observation of chiral magnetic soliton lattice state in CrNb_3S_6 by coherent soft x-ray diffraction imaging," in *Proceedings of the International Conference on Strongly Correlated Electron Systems (SCES2019)* (The Physical Society of Japan, 2020), p. 011194.
- ³⁶V. Ukleev, Y. Yamasaki, O. Utesov, K. Shibata, N. Kanazawa, N. Jaouen, H. Nakao, Y. Tokura, and T.-H. Arima, "Metastable solitonic states in the strained itinerant helimagnet FeGe ," *Phys. Rev. B* **102**, 014416 (2020).
- ³⁷T. Honda, Y. Yamasaki, H. Nakao, Y. Murakami, T. Ogura, Y. Kousaka, and J. Akimitsu, "Topological metastability supported by thermal fluctuation upon formation of chiral soliton lattice in CrNb_3S_6 ," *Sci. Rep.* **10**, 18596 (2020).
- ³⁸S. Maleyev, "Cubic magnets with Dzyaloshinskii-Moriya interaction at low temperature," *Phys. Rev. B* **73**, 174402 (2006).
- ³⁹M. Halder, A. Chacon, A. Bauer, W. Simeth, S. Mühlbauer, H. Berger, L. Heinen, M. Garst, A. Rosch, and C. Pfleiderer, "Thermodynamic evidence of a second skyrmion lattice phase and tilted conical phase in Cu_2OSeO_3 ," *Phys. Rev. B* **98**, 144429 (2018).
- ⁴⁰A. Miyake, J. Shibuya, M. Akaki, H. Tanaka, and M. Tokunaga, "Magnetic field induced polar phase in the chiral magnet CsCuCl_3 ," *Phys. Rev. B* **92**, 100406 (2015).
- ⁴¹Y. Araki, T. Sato, Y. Fujima, N. Abe, M. Tokunaga, S. Kimura, D. Morikawa, V. Ukleev, Y. Yamasaki, C. Tabata *et al.*, "Metamagnetic transitions and magnetoelectric responses in the chiral polar helimagnet $\text{Ni}_2\text{InSbO}_6$," *Phys. Rev. B* **102**, 054409 (2020).
- ⁴²V. Ukleev, A. Magrez, and J. White (2025). "Data for chiral soliton lattice in the bulk magnetoelectric helimagnet Cu_2OSeO_3 ," *Zenodo*.